Perspective correct occlusion-capable augmented reality displays using cloaking optics constraints

Isela D. Howlett (SID Student Member)
Quinn Smithwick (SID Member)

***Abstract* —** Perspective-correct occlusion-capable augmented reality displays are generalized using an optical cloak constraint for ray transfer analysis or simulations; any ray entering the optical system exits at the height and angle as if it passed through empty space. We analyze several systems with two-lens, three-lens, and four-lens looped groups in inline, folded, and looped configurations. We design and demonstrate a four-lens folded optical cloak and a three-lens inverted cloak with an erecting prism.

Keywords — *augmented reality, occlusion, cloaking optics, perspective correct.*

DOI # 10.1002/jsid.545

1 Objective

Although there has been a recent revival of virtual reality, augmented reality (AR) is seen as potentially more impactful.[1] Virtual reality tends to be isolating, causing problems for navigating and socializing in the physical world. On the other hand, AR visually integrates synthetic content onto real-world scenery allowing annotation of and interaction with the physical world. In optical see-through AR, a beam combiner optically adds the light from a display imaged at infinity and the light from a view of the real-world.[2] For bright and cluttered backgrounds, this results in low-contrast and semi-transparent synthetic objects that cannot occlude physical objects and are not visually well integrated into the scene (Fig. 1). Any mechanism to add occlusion capability to an AR display should maintain a perspective correct view of the physical world to allow natural interaction and navigation.[3,4]

We propose an AR display using the principles of cloaking optics to provide an internal focal plane to place an occluder mask while providing a perspective correct view of the real-world and composited opaque synthetic content.

2 Background

In typical optical see-through AR displays, a beam combiner additively composites the direct real-world view with a collimated image of a display. To provide the AR display with the capability to visually occlude physical objects with a sharp synthetic object, the real-world should be imaged onto a focal plane where a collocated occluder mask is placed. A beam combiner additively composites synthetic imagery on a display optically collocated with occluder mask and imaged real-world scene. The combination of the synthetic image and masked real-world view is re-collimated to appear to be located at "infinity" for the viewer.

An afocal 4f relay would achieve this function; however, a single 4f relay inverts the image and also moves the viewpoint to the other side of the relay. The latter results in an incorrect perspective view, so objects will appear closer than they actually are and parallax of the real-world will be incorrect. An occlusion capable AR display, ELMO,[5,6] used a single 4f relay with a prism to erect the image; however, this results in a view offset longitudinally (due to the relay) and would not be perspective correct.

One previous occlusion capable AR display uses a two functional-lens group real-image Bravais system[7,8] to ideally collocate a 1:1 image and its object. The system is designed for a particular object distance. An AR display should work for all eye reliefs and viewing objects at all distances. An x-cube prism between the two-lens groups folds the path and erects the view. From their raytrace, corresponding input and output rays are at the same height and angle, so rays are horizontally transferred across the optical system. The horizontal transfer would result in incorrect perspective.

ELMO IV[9] uses two afocal 4f relays spaced by a sum of their focal lengths, resulting in an upright view. Maintaining correct perspective is handled by a looped optical path with an initial double-sided mirror to collocate the user's viewpoint and a virtual image of the relayed viewpoint.

We aim to generalize perspective correct occlusion-capable AR displays by describing the perspective correct condition as an optical cloak constraint for ray transfer analysis or numerical raytracing simulations. The optical cloak constraint states that for any ray that enters the optical system, it exits at the height and angle as if it passed through empty space irrespective of what path it takes through the optical system, including forming focal planes necessary for occluder masks, thus providing a correct perspective through the

Received 02/12/17; accepted 03/08/17.
The authors are with Disney Research, Glendale, CA USA; e-mail: isela.howlett@gmail.com.

FIGURE 1 — Non-occluded augmented reality image in a bright, cluttered scene.

system regardless of viewpoint. In ray transfer analysis, we equate the composite ABCD matrices of the optical system to the ABCD matrix of rays traversing in free space the length the system.[10]

For simplicity of analysis, the Rochester Optical Cloak[10] uses two inline afocal 4f relays appropriately spaced to meet the optical cloak constraint. The rays entering the system focus to a plane, then exit the system at a height and angle as if they pass through empty space; objects are hidden or "cloaked" by being placed outside the focused caustic in the system, which does not include the optical axis.

For our perspective correct occlusion-capable AR display, an occluder mask (e.g., transparent liquid crystal panel or transparency) is placed at the focal plane closest the input (towards the real-world scene), and a display (e.g., transparent organic light-emitting diode or a beam-combined liquid crystal display) at the focal plane closest to the viewer. Being perspective correct, the field of view is determined and limited by the length of the system and the aperture of the initial input element. Because the optical cloak system consists of two inline 4f systems, it is quite long resulting in a small field of view. We modified the optical cloak to include folded designs to increase the field of view.

The generalization allows us to create or optimize optical layouts for perspective correct occlusion AR displays including those that are not looped and/or do not have an obvious real-image relayed viewpoint.

3 Design

3.1 Purpose and procedure

3.1.1 Folded optical cloak

We modify the optical cloak system so that it may be folded while still maintaining the perspective correct viewpoint. For example, we can model a folded optical system of two spaced 4f relays using ray transfer ABCD matrices, equating the result to an ABCD matrix for a ray travelling through the inline distance, d, between the input and output lenses, and solve for the spacing between the two relay sets, t (Fig. 2; Appendix D).

$$\begin{bmatrix} 1 & 0 \\ -\frac{1}{f} & 1 \end{bmatrix}\begin{bmatrix} 1 & 2f \\ 0 & 1 \end{bmatrix}\begin{bmatrix} 1 & 0 \\ -\frac{1}{f} & 1 \end{bmatrix}\begin{bmatrix} 1 & t \\ 0 & 1 \end{bmatrix}\begin{bmatrix} 1 & 0 \\ -\frac{1}{f} & 1 \end{bmatrix}\begin{bmatrix} 1 & 2f \\ 0 & 1 \end{bmatrix}\begin{bmatrix} 1 & 0 \\ -\frac{1}{f} & 1 \end{bmatrix} \quad (1)$$
$$= \begin{bmatrix} 1 & d \\ 0 & 1 \end{bmatrix}, \text{with } t = d + 4f.$$

For more complicated folded optical cloak systems, constrained optimization can be performed in numerical raytracing packages (e.g., Zemax) to find the required spacing or lens powers satisfying the optical cloak constraint between a set of representative input and output rays.

3.1.2 Inverted optical cloak with prism derotation

Although a standard optical cloak requires a minimum of four lenses to provide an erect perspective correct image of the real-world scene[10] because of one of the relay sets inverting/reverting the image to be upright and properly oriented, two-lens and three-lens systems can also be designed using ray transfer analysis that create perspective correct systems with an inverted cloak (Fig. 3). Prims can then be used to erect the image. Use of prisms to erect the image removes a relay set resulting in a compact system.

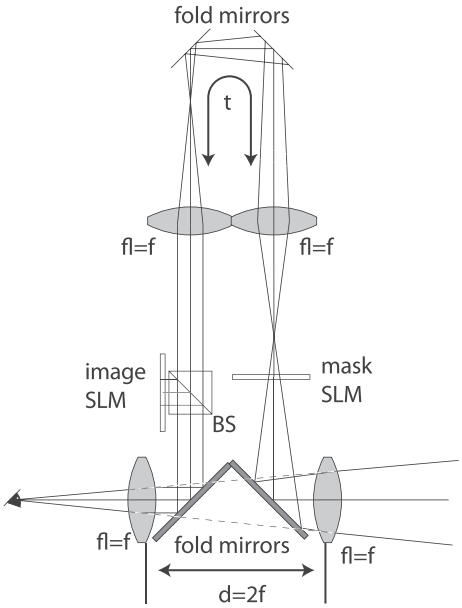

FIGURE 2 — Folded optical cloak augmented reality.

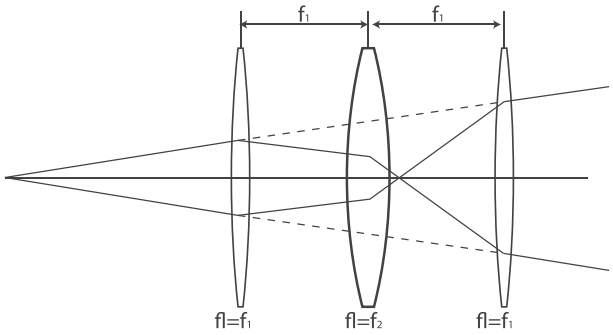

FIGURE 3 — Inverted optical cloak augmented reality.

$$\begin{bmatrix} 1 & 0 \\ -\frac{1}{f_1} & 1 \end{bmatrix}\begin{bmatrix} 1 & f_1 \\ 0 & 1 \end{bmatrix}\begin{bmatrix} 1 & 0 \\ -\frac{1}{f_2} & 1 \end{bmatrix}\begin{bmatrix} 1 & f_2 \\ 0 & 1 \end{bmatrix}\begin{bmatrix} 1 & 0 \\ -\frac{1}{f_1} & 1 \end{bmatrix}\begin{bmatrix} -1 & -t\cdot OPL \\ 0 & -1 \end{bmatrix} \quad (2)$$
$$= \begin{bmatrix} 1 & 2f_1 + t \\ 0 & 1 \end{bmatrix} \text{with } f_2 = \frac{f_1^2}{4f_1 - (nOPL - 1)\cdot t}$$

where f_1 is the focal length of the first and last lenses, f_2 is the focal length of the field lens, t is the prism geometric length, and OPL is the prism's normalized optical path length (Appendix A, C1).

A two-lens inline system cannot meet the cloaking criteria and be perspective correct without a prism or optical delay line outside the two lenses. This system is highly constrained leading to inflexible system design requirements (Appendix B1). A three-lens inline system can also meet the cloaking constraint and be perspective correct, with the focal length of the field lens providing an extra degree of freedom for more flexible designs (Appendix C1).

3.2 Implementation

3.2.1 Looped optical cloak

We made several prototypes of folded, looped (Fig. 4a,b) and an inverted optical cloak with an erecting prisms (Fig. 5a,b). For the looped optical cloak system, we started with a looped two 4f relay system using all fl = 75 mm, 50-mm OD lenses, with the inline distance of t = 75 mm being between the first and last refracting surfaces separated by a double-sided fold mirror. The distance between the two relay systems was d = 5 f. For an eye relief of 25 mm, the ray bundles, and field

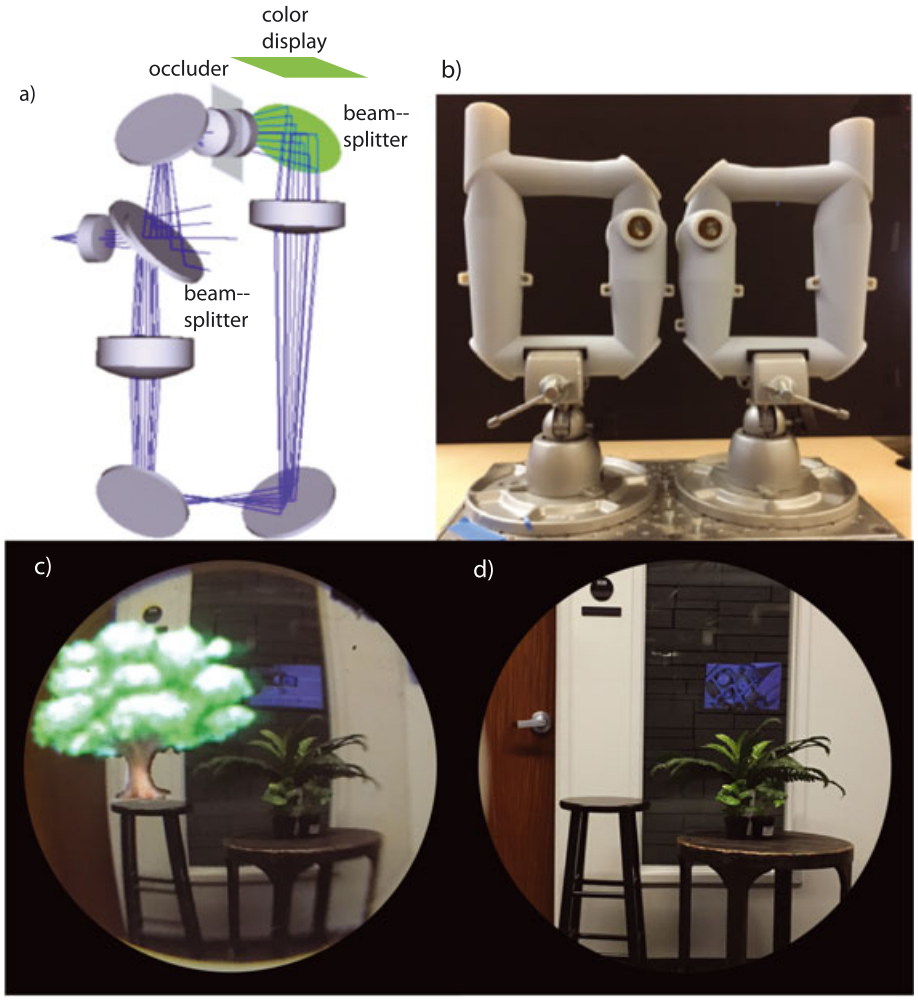

FIGURE 4 — Folded optical cloak augmented reality display. a) Zemax raytrace, b) prototype, c) occluded augmented reality view, and d) direct view.

of view was limited to 15° by the aperture of the second lens of the first relay.

To increase the field of view, the first lens was moved into the fold, so the double-sided mirror and last lens are the only inline elements, with a separation of t = 25 mm (Fig. 4a). It was desirable to keep the final lens inline, because the further away the final lens is from the viewpoint, the larger the view bundle in the optical system and the more likely it is to vignette and limit the field of view. Placing the object side lens into the fold allows the view to grow and fill the inline two-sided mirror and removes the additional inline length from the mirror to the second lens, which also reduces the spacing between the relays to meet the cloaking condition. The eye piece relay was modified to include fl = 30 and fl = 75 mm lens pairs, while the incoming relay is composed of fl = 30, fl = −50, and fl = 100 mm lenses. The modification of the incoming relay allows for the view bundle size to be reduced and to compress and constrain the ray bundles, so the eye lens was the limiting aperture. This maximizes the field of view for an eye-relief between 18 and 25 mm from the eye lens. Commercial lens prescriptions, used in place of the paraxial optics, allow the spacing of the lenses to be optimized in Zemax such that the field of view was the greatest and the optical cloak constraint was met. The optical componets are encased in a 3-D-printed shell (Connex 500 Objet3 Vero Gray material). A transparency placed at the first focal plane acted as an occluder masks. The folding design included a beam splitter in place of one of the fold mirrors, so an image source (i.e., mobile phone display) can be colocated with a focal plane and its image combined with the occluded real-world image. Two systems were made to create a stereoscopic AR display. This design was modified for increase field of view, but not for distortion or other aberration correction.

3.2.2 Inverted optical cloak with erecting prism

The paraxial design for the inverted optical cloak with erecting prism system uses fl = 50 mm, 25 mm OD lenses for the first and final lenses, separated by 100 mm. A Schmidt–Pechan prism is used for image erection. Design using ABCD matrices leads to the calculation of a field lens with fl = 16.13 mm to meet the optical cloak constraint (Fig. 4a). The fl = 50 mm paraxial lenses are exchanged for real lens specifications of Thorlabs AC254-050-A lenses, and the distances are changed to account for the real back focal distances. The field lens is constructed as a compound two-lens equivalent. Applying the 30-mm focal length lenses in place of the paraxial component, optimization leads to lens pair spacing of 5.149 mm resulting in a focal length of 16.86 mm when accounting for the real lens thicknesses. A transparency located at the focal plane between the field lenses was used as the occluder mask. An economy beam splitter is added between the first lens and the field lens, to allow the color image from a mobile phone to be composited. This setup produces an inverted and reverted image for the user to view. To correct this flip, a Schmidt–Pechan prism is placed between the eye and the eye lens. This design was not optimized for the field of view and the size of the occluder or display. The viewed scene includes physical objects multiple depths of 6′ and 12′ away.

3.3 Results

3.3.1 Looped optical cloak

The looped optical cloak has a 30° field of view for a viewpoint and eye relief of 25 mm. The perspective viewed through the system is correct. Physical objects appear with a 1:1 magnification (Fig. 4c,d). and the viewer is able to naturally focus on objects at different depths. Although some barrel distortion is present, the left and right eye images can be easily fused with correct and matching accommodation cues. The mask occludes the background, and the synthetic color image is superimposed (Fig. 4c) and appears in focus at the far background. The composited stereo image exhibits dark colors and tones in the shadows, usually not possible with see-through AR, resulting in high-contrast opaque imagery. Further lens design in conjunction with using optics simulation software to meet the cloak condition can reduce optical aberrations.

Notice that the ELMO IV system is a special case of a cloaked system with d = 0 and t = 2f, because the mirror is the only inline surface, and the spacing before the first lens is 3f/2 and f/2 before the last lens (Appendix E). This configuration may not always be desirable, because the further away the last (eyepiece) lens is from the system output (e.g., double-sided mirror), the larger the view bundle in the optical system and the more likely it is to vignette and limit the field of view. Also, the image of the viewpoint may not always be easily determined, making collocating the viewpoint and its image difficult. The use of the optical cloak constraint and optimization in our ray tracing package allowed us to solve for a different configuration including one inline lens, scaling relays and a field lens to increase our field of view.

3.3.2 Inverted optical cloak with erecting prism

The inverted optical cloak with erecting prism has a 7° field of view for an eye relief of 25 mm. The mask occludes the background, and the synthetic color image is superimposed. The perspective is correct, and near and far objects appear unchanged (Fig. 5d,e). As the eye relief varies, the perspective remains correct, but the field of view through the system changes as expected.

A Schmidt–Pechan prism from a pair of Nikon binoculars was used to erect the image. The prism was modeled both as an ABCD matrix (Fig. 5b) and as a non-sequential object from the ZEMAX object catalog (Fig. 5c). The ABCD matrix method shows that the cloaking condition can be met with the

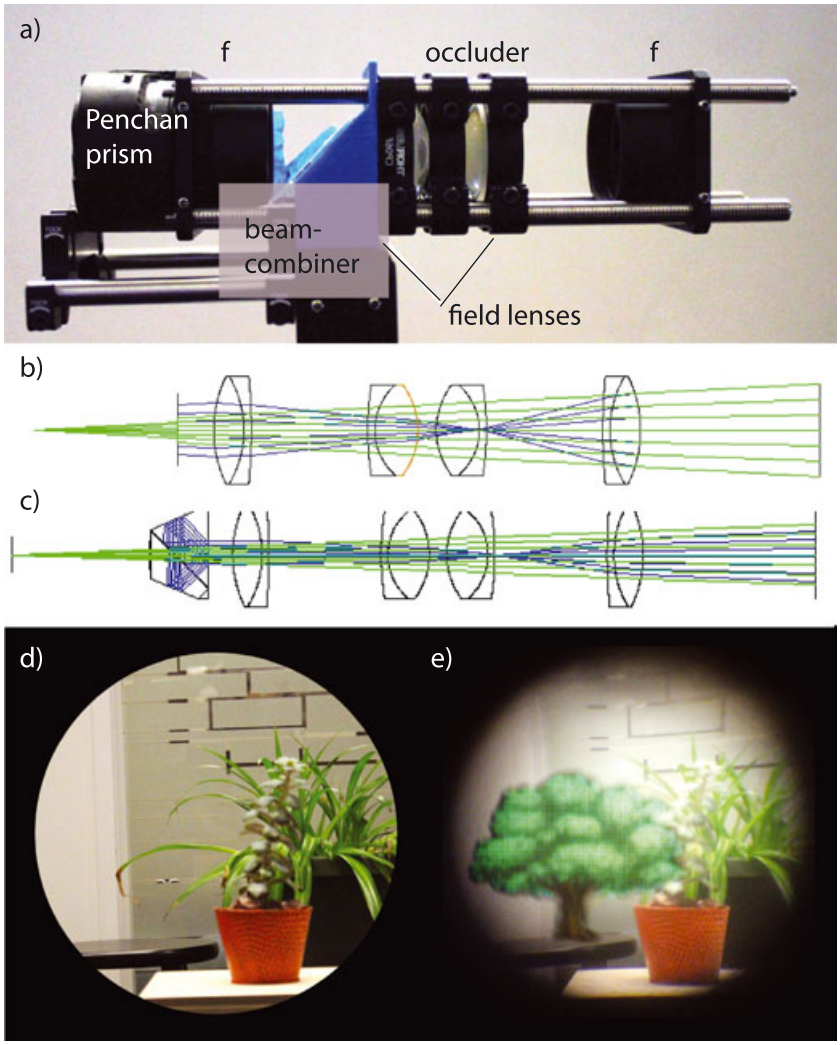

FIGURE 5 — Inverted optical cloak augmented reality (AR) display. a) Prototype, b) raytrace with ABCD prism, c) raytrace with Penchan prism, d) AR view, and e) occluded AR view.

correct OPL of the prism. In the figure, the ABCD matrix places the entrance and exit pupil of the prism as a paraxial element, which causes the sudden change of ray height at the prism. When modeling the prism with the non-sequential surface, the binocular's encased prism size is estimated as well the glass type. The built-in prism model is scaled to 7× the original size, and silica is used as the glass type. From the model, there are still some unknown parameters for the Nikon prism pair; this leads to a non-ideal perspective correct system in the model. However, experimentally, the placement of the field lenses was able to be adjusted to correct for the unknown distances.

The prism caused vignetting creating a smaller field of view than is possible with the lens group only. Larger prisms would reduce vignetting; however, we did not optimize this system for its field of view (Appendix C1). Another configuration using a Dove–Harting prism array was assembled and tested. Its shorter normalized optical path length provided a larger field of view (10°) than the Schmidt–Pechan; however, this Dove–Harting prism array has a slight vertical viewpoint shift, and there are seams from the prism interfaces.

Because these are inline systems, there are long distances between the first elements (prism) and the last (final lens), resulting in a small fields of view. A folded system would be more compact and potentially provide a larger field of view. The three-lens system with an x-cube prism would be shorter and increase the field of view. The use of three lenses makes this system perspective correct (Appendix C2) for all eye reliefs and for viewing objects at all distances, because it meets the cloaking condition. A two-lens folded system with an x-cube prism to fold the path and erect the image (*ala'* the real-image Bravais system) does not meet the cloaking constraint (Appendix B2).

It can be shown that a looped two-lens system is possible using an erecting prism and one relay with a looping mirror system to place the relayed real image at the object (*ala'* the ELMO system); however, the looping mirror system would make it bulky and cumbersome.

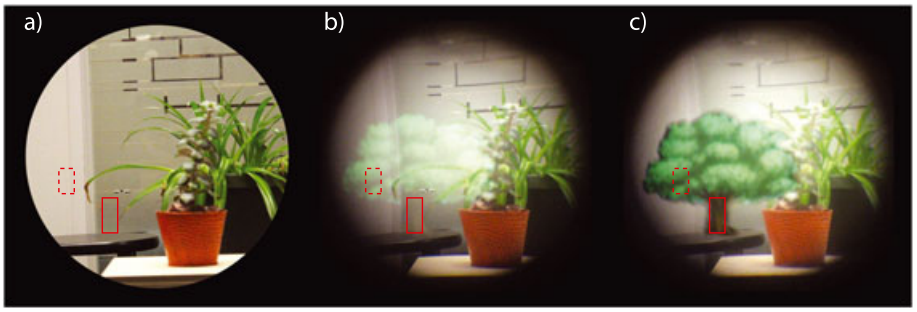

FIGURE 6 — Evaluation of the contrast of the augmented reality (AR) view (a), non-masked AR image (b), and a masked AR image (c). Two regions are selected for contrast evaluation, the window area (solid rectangle) with the AR tree trunk and the white wall area (dashed rectangle) with the AR leaves and branches.

TABLE 1 — Evaluation of pixel values to determine contrast from image regions in Fig. 6.

	Window/tree trunk			White wall/leaves		
Image	Min	Max	Contrast (%)	Min	Max	Contrast (%)
a)	33	216	73.49	171	219	12.31
b)	29	190	73.52	84	235	47.34
c)	6	148	92.21	14	230	88.52

Evaluating the background and contrast in the AR image shows increased contrast capabilities when the occlusion mask is used. The contrast is measured using the pixel values of select regions in the image, $C = \frac{I_{max} - I_{min}}{I_{max} + I_{min}}$. The two regions selected in the AR views in Fig. 6 are the tree trunk in the window section (solid rectangle) and the leaves in the white wall section (dashed rectangle). ImageJ[11] is used to stack the selected image and measure the pixel values from the same location in each image. The resulting minimum, maximum, and contrast values are provided in Table 1.

The overall improvement when the mask is in place is apparent with contrast values of 92.21% and 88.52% the window and white wall, respectively. The non-masked AR image provides values of 73.52% and 47.34% for the same regions. The non-masked image for the case of a darker window background, the change in the image contrast between the original image and the non-masked AR image, is negligible, leading to the trunk of the AR tree having similar contrast as the window itself.

4 Impact

The cloaking constraint allows us to create or optimize optical layouts for perspective correct occlusion AR displays using ray transfer analysis or constrained optimization in ray tracing simulations. The system does not need to be designed for particular object distances or eye relief. By generalizing the requirements of a perspective correct occlusion-capable AR display using the cloaking condition, we are able to analyze and design several systems including two-lens, three-lens, and four-lens group systems with inline, folded, and looped configurations. Building upon the optical cloak constraint, we will further explore techniques to increase field of view while achieving a compact form factor.

Acknowledgment

The authors would like to thank Bobby Bristow for his knowledge and time when fabricating the 3-D printed components for this work.

Appendices:

A. Normalized Optical Path Length for Pechan Prism

For the raytrace analysis, we are interested in finding the normalized optical path length (OPL) for an inline erecting prism to fold the optical path and erect the view in two-lens and three-lens optical cloak systems. The OPL is the ratio of the folded optical path in the prism's medium and the free-space path length between the prism's input and output planes. Different inline erecting prisms of length d will have different OPLs, but their ABCD matrix will generally fit the form of $\begin{bmatrix} -1 & -d \cdot OPL \\ 0 & -1 \end{bmatrix}$. To determine the OPL of a particular prism, we shall use ray transfer analysis. One such prism is the Schmidt–Pechan prism, constructed using a combination of a half-penta prism and a Schmidt prism. For our purposes, we can model the prism as a set of sequential mirrors embedded in a medium of refraction index n and follow the path of the optical axis through the prism. For this analysis, the chief ray travels $\frac{2}{5}d$ from prism's front face to reflect off the main 45° mirror, $\frac{3}{5}d$ to the bottom 67.5° mirror, $\frac{3\sqrt{2}}{5}d$ to the prism's vertical back face, $\frac{3\sqrt{2}}{5}d$ to the top 67.5° mirror, $\frac{3}{5}d$ to the back of the 45° mirror then travels $\frac{3}{5}d$ to pass through the prism's back face.

$$\begin{bmatrix}1 & 0\\ 0 & n\end{bmatrix}\begin{bmatrix}1 & \frac{3}{5}d\\ 0 & 1\end{bmatrix}\begin{bmatrix}-1 & 0\\ 0 & -1\end{bmatrix}\begin{bmatrix}1 & \frac{3}{5}d\\ 0 & 1\end{bmatrix}\begin{bmatrix}-1 & 0\\ 0 & -1\end{bmatrix}\begin{bmatrix}1 & \frac{3\sqrt{2}}{5}\\ 0 & 1\end{bmatrix}\begin{bmatrix}-1 & 0\\ 0 & -1\end{bmatrix}\begin{bmatrix}1 & \frac{3\sqrt{2}}{5}d\\ 0 & 1\end{bmatrix}\begin{bmatrix}-1 & 0\\ 0 & -1\end{bmatrix}\begin{bmatrix}1 & \frac{3}{5}d\\ 0 & 1\end{bmatrix}\begin{bmatrix}-1 & 0\\ 0 & -1\end{bmatrix}\begin{bmatrix}1 & \frac{2}{5}d\\ 0 & 1\end{bmatrix}\begin{bmatrix}1 & 0\\ 0 & \frac{1}{n}\end{bmatrix} \quad (A.1)$$

$$= \begin{bmatrix}-1 & -\frac{d(11+6\sqrt{2})}{5n}\\ 0 & -1\end{bmatrix}$$

The OPL is therefore

$$OPL_{pechan} = \frac{(11+6\sqrt{2})}{5n} \quad (A.2)$$

Using the index of refraction for glass, $n = 1.5$ gives an $OPL_{pechan} = 2.60$. An object that passes through a Schmidt–Pechan prism will appear as an inverted image 2.60 times the prism's depth further away than without a prism. The OPL of other prisms and variations can be solved in a similar manner.

B1. Inline Two-Lens System Analysis

The optical constraint condition for a generic two-lens inline system with an erecting prism is described by equating the concatenated ABCD matrices of an erecting prism of length, d, and optical path length, $d \cdot OPL$, and two lenses of focal lengths, f_1 and f_2, separated by a distance, t, to the ABCD matrix for a ray travelling the distance between the prism input and last lens $d + t$ in free space (Fig. A1).

$$\begin{bmatrix}1 & 0\\ -\frac{1}{f_1} & 1\end{bmatrix}\begin{bmatrix}1 & t\\ 0 & 1\end{bmatrix}\begin{bmatrix}1 & 0\\ -\frac{1}{f_2} & 1\end{bmatrix}\begin{bmatrix}-1 & -d\cdot OPL\\ 0 & -1\end{bmatrix} = \begin{bmatrix}1 & d+t\\ 0 & 1\end{bmatrix} \quad (B1.1)$$

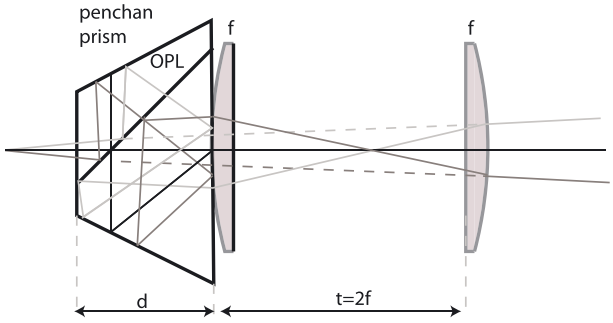

FIGURE A1 — Two-lens with erecting prism.

Simplifying

$$\begin{bmatrix}-\frac{f_2 - t}{f_2} & -\frac{(f_2 - t)\cdot OPL\cdot d + t\cdot f_2}{f_2}\\ -\frac{-t + f_1 + f_2}{f_1 f_2} & -\frac{(-t + f_1 + f_2)\cdot OPL\cdot d - (-t + f_1)f_2}{f_1 f_2}\end{bmatrix} = \begin{bmatrix}1 & d+t\\ 0 & 1\end{bmatrix} \quad (B1.2)$$

Solving this set of equations gives $f = f_1 = f_2$, $t = 2f$, and $d = \frac{4f}{(OPL-1)}$.

Although this system meets the optical constraint, it is not very flexible in its design. For two lenses must be the same focal length, f; and the spacing and prism depth (which is also constrained by its OPL based on its type) are both constrained by f. The depth of the prism is almost as deep as the spacing between the lenses. This also constrains the depth of the entire system and hence the field of view. The optical delay of the prism outside the lens pair is required for an inline two-lens system to meet the optical cloaking constraint.

B2. Folded Two-Lens System Analysis

Here, we show that a folded system using two-lens groups (objective and eyepiece) is not a perspective correct system satisfying the optical constraint condition. An example, we analyze a two-lens system each of focal length, f, with an x-cube prism of index of refraction n, depth, d, and folded path length, $2L$, between them (acting as both an erector and fold mirrors) and a reflective occluder at the focal plane.

The optical constraint condition using ray transfer analysis for this system is as follows.

$$\begin{bmatrix}1 & 0\\ -\frac{1}{f} & 1\end{bmatrix}\begin{bmatrix}1 & 0\\ 0 & n\end{bmatrix}\begin{bmatrix}1 & L\\ 0 & 1\end{bmatrix}\begin{bmatrix}-1 & 0\\ 0 & -1\end{bmatrix}\begin{bmatrix}1 & L\\ 0 & 1\end{bmatrix}\begin{bmatrix}1 & 0\\ 0 & \frac{1}{n}\end{bmatrix}\begin{bmatrix}1 & 0\\ -\frac{1}{f} & 1\end{bmatrix} \quad (B2.1)$$

$$= \begin{bmatrix}1 & d\\ 0 & 1\end{bmatrix}$$

Simplifying

$$\begin{bmatrix} \dfrac{-f+2\cdot\frac{L}{n}}{f} & -2\cdot\dfrac{L}{n} \\ \dfrac{2\cdot f-2\cdot\frac{L}{n}}{f^2} & \dfrac{-f+2\cdot\frac{L}{n}}{f} \end{bmatrix} = \begin{bmatrix} 1 & d \\ 0 & 1 \end{bmatrix} \tag{B2.2}$$

Solving for L and d gives

$$L = fn \quad d = -2f \tag{B2.3}$$

L and d are both distances; however, from Eq. [(B2.3)], they have opposite signs so one must be negative. We cannot have a negative distance, so this configuration of a two-lens system with an x-cube prism between the lenses does not meet the cloaking constraint.

C1. Compact Optical Cloak System (Three-lens) Analysis

Here, we show that a three-lens system with an erecting prism meets the optical cloak constraint and produces a perspective correct system.

The optical cloaking constraint for this system is described by equating the concatenated ABCD matrices of an erecting prism of length, t, and normalized optical path length, OPL, two lenses of equal focal lengths, f_1, separated by a distance $2f_1$, with a field lens (located at the focal plane of the two previous lenses) of focal length f_2, to the ABCD matrix for a ray travelling a distance equal to twice the focal length f_1 plus the thickness of the prism, t, in free space

$$\begin{bmatrix} 1 & 0 \\ -\frac{1}{f_1} & 1 \end{bmatrix}\begin{bmatrix} 1 & f_1 \\ 0 & 1 \end{bmatrix}\begin{bmatrix} 1 & 0 \\ -\frac{1}{f_2} & 1 \end{bmatrix}\begin{bmatrix} 1 & f_1 \\ 0 & 1 \end{bmatrix}\begin{bmatrix} 1 & 0 \\ -\frac{1}{f_1} & 1 \end{bmatrix}\begin{bmatrix} -1 & -t\cdot OPL \\ 0 & -1 \end{bmatrix} = \begin{bmatrix} 1 & 2f_1+t \\ 0 & 1 \end{bmatrix} \tag{C1.1}$$

Simplifying the left hand side of the equation (LHS)

$$\begin{bmatrix} 1 & \dfrac{t\cdot OPL\cdot f_2 - f_1(2f_2 - f_1)}{f_2}\cdot \\ 0 & 1 \end{bmatrix} = \begin{bmatrix} 1 & 2f_1+t \\ 0 & 1 \end{bmatrix} \tag{C1.2}$$

Solving for f_2 results in

$$f_2 = \frac{{f_1}^2}{4f_1 - (OPL-1)\cdot t} \tag{C1.3}$$

We conclude that this three-lens system with a field lens of the focal length given by Eq. [(C1.3)] satisfies the cloaking constraint. We can split the field lens, which gives this system an accessible focal plane, allowing it to be used as a perspective correct occlusion capable AR display. Compared with the two-lens inline cloak, we have more flexibility in the design, because we can choose different combinations of f_1 and t, and then f_2 can be found to meet the optical cloak constraint.

This system can also be used as a three-lens optical cloak to hide objects outside the system's caustic.

C2. X-Cube Prism Three-Lens System Analysis

Although the folded two-lens system with an x-cube prism is not perspective correct, we show that a three-lens system with an x-cube erector prism is perspective correct, which could lead to a very compact perspective correct occlusion capable system. This system consists of two lenses each of focal length f with an x-cube prism of index of refraction n, depth, d, and folded path length, $2L$, between them (acting as both an erector and fold mirrors) and a field lens of focal length, f_2, and a reflective occluder at the focal plane (Fig. A2).

$$\begin{bmatrix} 1 & 0 \\ -\frac{1}{f} & 1 \end{bmatrix}\begin{bmatrix} 1 & 0 \\ 0 & n \end{bmatrix}\begin{bmatrix} 1 & L \\ 0 & 1 \end{bmatrix}\begin{bmatrix} 1 & 0 \\ 0 & \frac{1}{n} \end{bmatrix}\begin{bmatrix} 1 & 0 \\ -\frac{1}{f_2} & 1 \end{bmatrix}\begin{bmatrix} -1 & 0 \\ 0 & -1 \end{bmatrix}\begin{bmatrix} 1 & 0 \\ -\frac{1}{f_2} & 1 \end{bmatrix} \tag{C2.1}$$

$$\begin{bmatrix} 1 & 0 \\ 0 & n \end{bmatrix}\begin{bmatrix} 1 & L \\ 0 & 1 \end{bmatrix}\begin{bmatrix} 1 & 0 \\ 0 & \frac{1}{n} \end{bmatrix}\begin{bmatrix} 1 & 0 \\ -\frac{1}{f} & 1 \end{bmatrix} = \begin{bmatrix} 1 & d \\ 0 & 1 \end{bmatrix}$$

$$\begin{bmatrix} \dfrac{\left(-f_2+2\cdot\frac{L}{n}\right)\cdot f+2\cdot\frac{L}{n}\cdot\left(f_2-\frac{L}{n}\right)}{ff_2} & \dfrac{2\cdot\frac{L}{n}\cdot\left(f_2-\frac{L}{n}\right)}{f_2} \\ \dfrac{2\left(f-\frac{L}{n}\right)\left(f_2+f-\frac{L}{n}\right)}{f^2\cdot f_2} & \dfrac{\left(f_2-2\cdot\frac{L}{n}+f\right)\frac{L}{n}-\left(f-\frac{L}{n}\right)\cdot f_2}{ff_2} \end{bmatrix} = \begin{bmatrix} 1 & d \\ 0 & 1 \end{bmatrix} \tag{C2.2}$$

Letting $d = f$ for a cube prism, and solving for L and f_2 gives

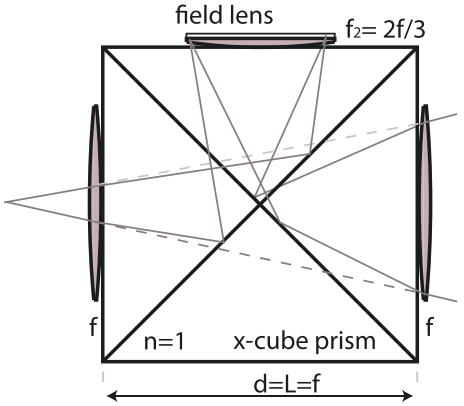

FIGURE A2 — Three-lens x-prism.

$$L = fn \text{ and } f_2 = \frac{2}{3}f \tag{C2.3}$$

The third lens is a field lens of focal length f_2 with a reflective Spatial Light Modulator (SLM) at the focal plane acting as an occluder. Light transverses the field lens twice.

D. Folded Optical Cloak System (Four-lens) Analysis

Here, we show that a folded four-lens system can meet the optical cloak constraint and produce a perspective correct system with an accessible real image plane for adding an occluder. We model a folded optical system of two spaced 4*f* relays (two lenses of focal length *f* spaced 2*f* apart) using ray transfer ABCD matrices, equating the result to an ABCD matrix for a ray travelling through the inline distance, *d*, between the input and output lenses, and solve for the spacing between the two relay sets, *t* (Fig. 2).

$$\begin{bmatrix} 1 & 0 \\ -\frac{1}{f} & 1 \end{bmatrix}\begin{bmatrix} 1 & 2f \\ 0 & 1 \end{bmatrix}\begin{bmatrix} 1 & 0 \\ -\frac{1}{f} & 1 \end{bmatrix}\begin{bmatrix} 1 & t \\ 0 & 1 \end{bmatrix}\begin{bmatrix} 1 & 0 \\ -\frac{1}{f} & 1 \end{bmatrix}\begin{bmatrix} 1 & 2f \\ 0 & 1 \end{bmatrix}\begin{bmatrix} 1 & 0 \\ -\frac{1}{f} & 1 \end{bmatrix} = \begin{bmatrix} 1 & d \\ 0 & 1 \end{bmatrix} \tag{D.1}$$

Simplifying the LHS

$$\begin{bmatrix} 1 & t-4f \\ 0 & 1 \end{bmatrix} = \begin{bmatrix} 1 & d \\ 0 & 1 \end{bmatrix} \tag{D.2}$$

Solving for *t*, the spacing between the two relay sets,

$$t = d + 4f \tag{D.3}$$

E. ELMO as a Looped Optical Cloak System Analysis

The ELMO system consists of a double-sided mirror, with two 1:1 magnification 4*f* relays, each with lenses of focal length *f* spaced 2*f* apart. The two relays are spaced a distance 2*f* apart. The mirror is the only inline surface (so the inline distance, *d*, equals 0), and there is a spacing of 3*f*/2 between the mirror and the first lens and a spacing of *f*/2 after the last lens to the mirror. This configuration allows the optical path to form a loop, so a real image of the viewpoint is relayed around the loop and before the mirror, allowing a virtual image of the viewpoint in the mirror to be collocated with the actual viewpoint. The resulting ray transfer matrix is in an identity matrix, so all rays from one side of the mirror appear at the same height and angle on the other side of the mirror.

$$\begin{bmatrix} 1 & \frac{f}{2} \\ 0 & 1 \end{bmatrix}\begin{bmatrix} 1 & 0 \\ -\frac{1}{f} & 1 \end{bmatrix}\begin{bmatrix} 1 & 2f \\ 0 & 1 \end{bmatrix}\begin{bmatrix} 1 & 0 \\ -\frac{1}{f} & 1 \end{bmatrix}\begin{bmatrix} 1 & 2f \\ 0 & 1 \end{bmatrix}\begin{bmatrix} 1 & 0 \\ -\frac{1}{f} & 1 \end{bmatrix} \cdot \begin{bmatrix} 1 & 2f \\ 0 & 1 \end{bmatrix}\begin{bmatrix} 1 & 0 \\ -\frac{1}{f} & 1 \end{bmatrix}\begin{bmatrix} 1 & \frac{3f}{2} \\ 0 & 1 \end{bmatrix} = \begin{bmatrix} 1 & 0 \\ 0 & 1 \end{bmatrix} \tag{E1}$$

References

1 A. Charlton, "Tim Cook and Apple prefer AR over VR because it allows human contact," *International Business Times* (2016). [Online]. Available: http://www.ibtimes.co.uk/tim-cook-reveals-why-apple-prefers-augmented-reality-vr-1586408.

2 J. Zhou, Calibration of optical see through head mounted displays for augmented reality. ProQuest, East Lansing, (2007) Print.

3 A. H. Behzadan *et al.*, "Augmented reality visualization: a review of civil infrastructure system applications," *Adv. Eng. Informatics*, **29**, No. 2, 252–267 (2015).

4 D. Baricevic *et al.*, "A hand-held AR magic lens with user-perspective rendering," *2012 IEEE International Symposium on Mixed and Augmented Reality (ISMAR)* (2012), pp. 197–206.

5 K. Kiyokawa *et al.*, "ELMO: an enhanced optical see-through display using an LCD panel for mutual occlusion," (2001a).

6 K. Kiyokawa *et al.*, "An optical see-through display for mutual occlusion with a real-time stereovision system," *Computers & Graphics*, **25**, No. 5, 765–779 (2001b).

7 O. Cakmakci *et al.*, "Design of a compact optical see-through head-worn display with mutual occlusion capability." *Novel Optical Systems Design and Optimization VIII* (2005).

8 O. Cakmakci *et al.*, "A compact optical see-through head-worn display with occlusion support," *Third IEEE and ACM International Symposium on Mixed and Augmented Reality* (2004).

9 K. Kiyokawa *et al.*, "An occlusion capable optical see-through head mount display for supporting co-located collaboration," *The Second IEEE and ACM International Symposium on Mixed and Augmented Reality, 2003. Proceedings* (2003), pp. 133–41.

10 J. S. Choi *et al.*, "Paraxial Ray Optics Cloaking," *Opt. Express*, **22**, No. 24, 29465 (2014).

11 C. A. Schneider, W. S. Rasband and K. W. Eliceiri, "NIH Image to ImageJ: 25 years of image analysis," *Nat. Methods*, **9**, No. 7, 671–675 (2012).

Isela D. Howlett is a graduate research associate at the University of Arizona in Tucson, Arizona. Her research with Disney Research Los Angeles was conducted during internships in 2014 and 2016. Her academic background includes a BS in Optical Sciences and Engineering from the University of Arizona, an MS in Electrical Engineering from Colorado State University, and she will receive her PhD in Optical Sciences on August 2017.

Quinn Smithwick is a Senior Research Scientist at Disney Research in Los Angeles, California. His main research area at Disney Research Los Angeles is novel display technologies with particular emphasis on autostereoscopic displays and augmented reality environments. He received his PhD in Aeronautics and Astronautics from the University of Washington for his dissertation on the nonlinear modeling and control of a miniature scanning endoscope. His postdoctoral research at Harvard Medical School was on the development of a transportable scanning laser ophthalmoscope. His postdoctoral research at the MIT Media Lab was on the development of MIT's next generation holographic video display. He joined Disney Research in 2010.